Transformation of Polyhedrons

Yan Chen[1,2*], Fufu Yang[1], Zhong You[1,3*]

Author affiliation:

[1] School of Mechanical Engineering, Tianjin University, Tianjin 300072, China

[2] Key Laboratory of Mechanism Theory and Equipment Design of Ministry of Education, Tianjin University, Tianjin 300072, China

[3] Department of Engineering Science, University of Oxford, Parks Road, Oxford, OX1 3PJ, UK

* Corresponding Authors:

Email: yan_chen@tju.edu.cn, ORCID ID: 0000-0002-4742-6944

zhong.you@eng.ox.ac.uk, ORCID ID: 0000-0002-5286-7218

Keywords:

Platonic solid; Archimedean solid; polyhedral transformation; 1-DOF kinematic motion; spatial linkage.

Abstract

Polyhedral transformation enables large volumetric change amongst Platonic and Archimedean solids. It has great potential for use in applications where transportability and protection of payload are critical design features, such as drug delivery capsules, satellites, or space habitats. However, the existing designs introduce many degrees of freedom, making it difficult or impossible to synchronise motion, and thus the practical applicability of mechanisms becomes restricted. This paper develops a kinematic method to enable polyhedral transformation with a single degree of freedom. The approach has been implemented for three sets of transformations, between truncated octahedron and cube, truncated tetrahedron and tetrahedron, and cuboctahedron and octahedron. Motion analysis indicates that transformation path is unique without singularity, which is further demonstrated with physical validation models. We envisage that our method could be suitable for extension to other paired polyhedron sets.

INTRODUCTION

In geometry, two important classes of convex polyhedrons consisting of regular polygonal faces with highly symmetrical geometry are the Platonic solids and Archimedean solids (*1*). The Platonic solids have only one type of regular polygonal face, which include five polyhedrons: tetrahedron, cube, octahedron, dodecahedron, and icosahedron, whereas the Archimedean solids are composed of more than one type of regular polygonal faces, which have thirteen polyhedrons excluding the prisms and antiprisms. Hollow polyhedrons of the two families can transform from one to the other if two paired polyhedrons comprise the same number of identical-type polygonal faces. Figure 1 shows three such pairs, and it is possible, for instance, to transform a cuboctahedron to an octahedron for both polyhedrons have eight triangular faces. The identical faces remain rigid during the transformation whilst the other faces vanish. The volumetric expansion ratios of the transformation are 23, 5, and 11.3, respectively, for the three paired polyhedrons shown in Fig. 1.

Not only are transformable polyhedrons mathematically interesting, but they also have many potential applications, e.g., they form perfect habitats for space travel which have growth capability (*2*), and they may be used to package a CubeSat to a small volume for launch which then expand into a considerably large structure once it reaches the orbit. The rigid faces are ideal for mounting electronic devices such as solar panels (*3*).

Transformation of polyhedrons was first proposed by Buckminster Fuller (*4*). A comprehensive list was provided by Clinton (*5*). Such transformation involves rotation and translation of rigid faces. For example, in the transformation between an octahedron and a cuboctahedron, each triangular face is allowed to rotate and translate about its normal at the centre, and its connections with the neighbouring triangles are always maintained. This is kinematically equivalent to a system where each of eight triangles in cuboctahedron has its own cylindrical joint whose axis passes through both the centres of the triangles and that of the polyhedrons, and the triangles are connected by spherical joints (ball joints) at the polyhedral vertices. The system has one degree of freedom (DOF) provided that the axes of all cylindrical joints are fastened together at the centre of the polyhedron (SM: Video 1). This, however, makes the transformation of little practical use as the space enclosed by the faces is taken up by the physical joints. If the axes of the cylindrical joints were not physically fixed together, the system would have six DOFs, as demonstrated by Buckminster Fuller's own model (*6*), making it impossible to complete the transformation in an orderly way. Shim et. al. suggested to syncrinise the transformation by applying a uniformly distributed pressure (*7*). This approach, however, works only for polyhedrons made from relative soft materials and their behaviour becomes both material and loading dependent.

The above example demonstrates that it is extremely challenging to accomplish the transformation of polyhedrons mechanically. To date two engineering approaches have been proposed. A modified Buckminster Fuller's Jitterbug capable of performing

a symmetrical transformation between a regular octahedron and a cuboctahedron was fabricated at the Heureka Exposition in Zurich in 1991 (*8*) in which the cylindrical joints at the centres of the triangular faces were eliminated, and the spherical joints at vertices were replaced by universal joints. The resulted assembly had one DOF. Yet this approach cannot be extended to other paired polyhedrons as the numbers of DOFs would remain high (e.g., the truncated octahedron would end up with 18 DOFs). Verheyen (*9*) fabricated some Jitterbug-like polyhedrons where each triangular faces were made into two layers joined by a revolute joint (hinge joint), whereas the spherical joints at vertices remained. The resulted double layered structures were far too complex, and rather unstable during the transformation due to the existence of motion bifurcations.

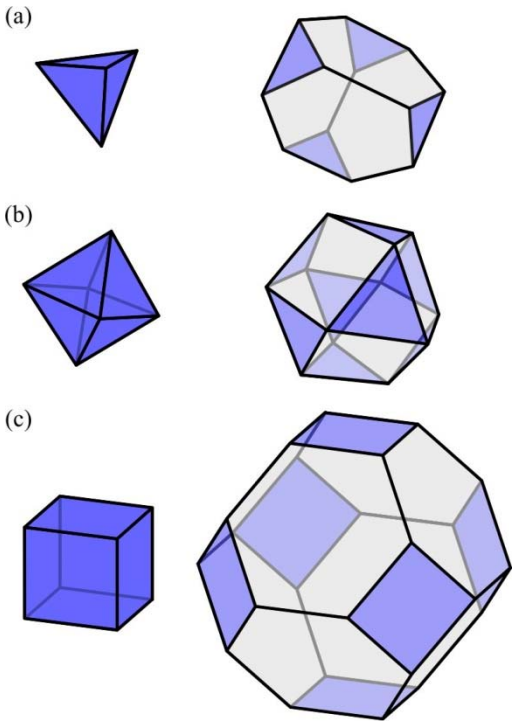

Fig. 1. Three paired Platonic and Archimedean polyhedrons. The common rigid faces are shaded in blue. (a) A tetrahedron and a truncated tetrahedron; (b) an octahedron and a cuboctahedron; and (c) a cube and a truncated octahedron. When transformations take place, the volumetric expansion ratios are 23, 5, and 11.3, respectively.

Apart from these two attempts, other transformable polyhedron models were also produced in which there were actually no shape transformation between a Platonic solid and an Archimedean solid. For instance, Agrawal et al. (*10*) constructed a 1-DOF expanding polyhedron by installing telescopic bars on each side of a polyhedron. The polyhedron preserved its shape when volumetric change took place. A toy known as the Switch Pitch (*11*) was generated using a centrally geared expanding mechanism

within the central void. Gosselin and Gagnon-Lachance (*12*), Laliberté and Gosselin (*13*), as well as Wei and Dai (*14*) proposed a number of expandable polyhedrons, but expansion ended up with irregular polyhedral shapes. Kiper and Söylemez (15) introduced the overconstrained Bennett linkage to regular polyhedrons, resulted in structures with a rather small expansion ratio.

A mechanical transformable polyhedron requires, first of all, the number of DOF to be low so that the transformation can be easily controlled, and secondly, the central void must not be taken up by complex joints or control systems. The limitations of existing concepts prompt us to devise an effective method to transform polyhedrons amongst paired Platonic and Archimedean solids with one DOF. This objective is achieved by the introduction of spatial linkages. Though the present paper focuses on three paired polyhedrons shown in Fig. 1, the concept can also be extended to other paired polyhedrons.

RESULTS AND DISCUSSION

Transformation between Truncated Octahedron and Cube

Both the truncated octahedron and cube are both octahedral symmetric (O_h) polyhedrons with 24 rotational symmetries (*16*). Let the sides of polyhedrons be a unit length, the positions of all vertices can be obtained using a Cartesian coordinate system shown in Figs. 2(a) and (b). After the transformation, each group of three vertices in truncated octahedron converge to a single vertex on the cube. Such a vertex-motion arrangement is unique if no interference occurs during the transformation. As a result, all of the eight hexagonal hollows will vanish after the transformation. If only spherical joints are used at all of the vertices, the truncated octahedron would have 18 DOFs, and thus, extra constraints must be imposed to reduce the number of DOFs. One approach is to replace the 3-DOF spherical joint with 1-DOF revolute joint. Each such replacement will in general reduce two DOFs according to the Kutzbach criterion (*17*). However, due to the high degree of symmetry in the truncated octahedron, it is not straight forward to get the true DOF simply by applying the Kutzbach criterion, which we shall elaborate further next.

Let us examine a single hollow, $A_1A_2C_1C_2B_1B_2$, Fig. 2(a), whose initial configuration is a regular hexagon. After transformation, vertices A_1, C_1 and B_1 converge to a single vertex on the cube, whilst A_2, C_2 and B_2 end up at the adjacent vertices of the cube, Fig. 2(b), and so do the vertices on the neighbouring hollows. Hence, the motion of hollow $A_1A_2C_1C_2B_1B_2$ will have threefold symmetry. We decide to use 1-DOF revolute joint at those vertices, and to enable the motion, the hollow must be a threefold-symmetric 6*R* Bricard linkage, which is made of six links connected by six revolute joints (hence 6*R*) forming a loop (*18*).

The Bricard linkage is an overconstrained linkage which has mobility only under strict geometrical conditions (*18*). These conditions are met by adjusting the orientation of each 1-DOF revolute joint. The rotational axes of the revolute joints of the threefold-symmetric Bricard linkage $A_1A_2C_1C_2B_1B_2$ can be determined based on the initial and final configurations on the paired polyhedrons, which is illustrated in Fig. 2(c). After transforming into cube, sides B_1C_2 and B_1B_4 must be collinear, which demands the revolute joint axis at B_1 be on the plane bisecting angle $\angle C_2B_1B_4$. Meanwhile, because of the threefold symmetry of the linkage, the same axis must be on the plane containing B_1, O and A_2. Thus, the direction of the revolute joint axis at B_1 is

$$\mathbf{s}_{B1} = (0, \sqrt{2}, \frac{\sqrt{2}}{2})^{\mathrm{T}}. \qquad [1]$$

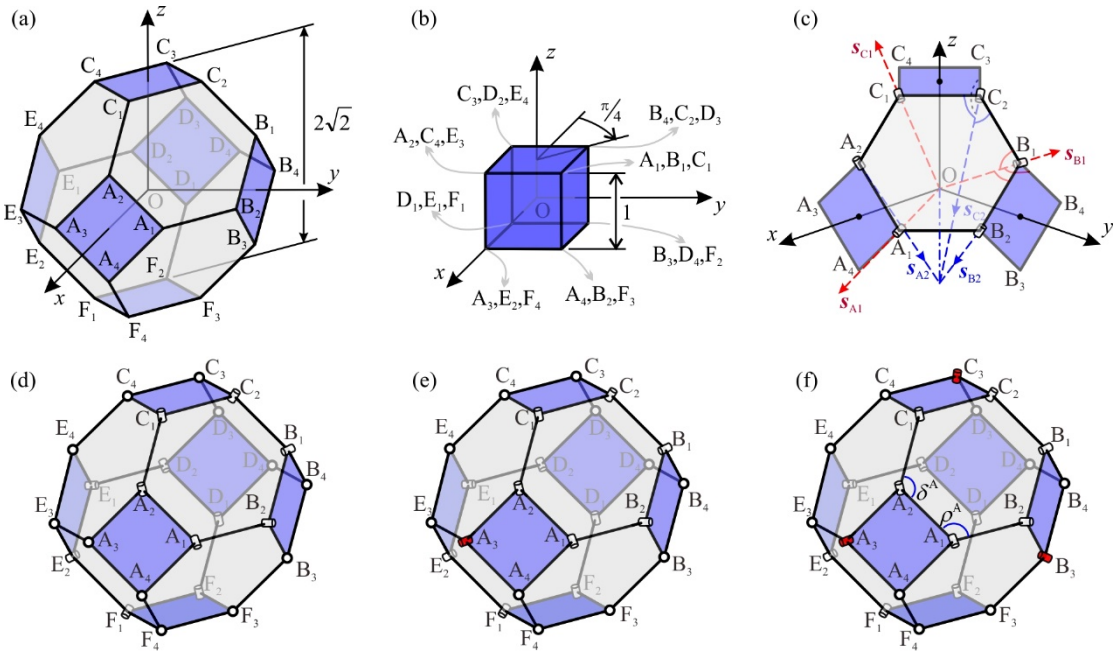

Fig. 2. Joint replacement and joint positions in the truncated octahedron and cube. (a) The truncated octahedron and the Cartesian coordinate system; (b) positions of the vertices when the truncated octahedron shrinks to a cube; (c) a threefold-symmetric 6*R* Bricard linkage is introduced to realize the transformation of three squares A, B, C, and axes of revolute joints; (d) a 2-DOF system is obtained after the introduction of two threefold-symmetric Bricard linkages $A_1A_2C_1C_2B_1B_2$ and $D_1D_2E_1E_2F_1F_2$; (e) spherical joint at vertex A_3 is replaced with a revolute joint (shown in red) to obtain a 1-DOF system; (f) the same replacement takes place at vertices B_3 and C_3 whilst the system remains one DOF.

Similarly, the revolute axes at A_1 and C_1 can be set as

$$\mathbf{s}_{A1} = (\sqrt{2}, \frac{\sqrt{2}}{2}, 0)^T,\ \mathbf{s}_{C1} = (\frac{\sqrt{2}}{2}, 0, \sqrt{2})^T. \quad [2]$$

These axes all point towards the centres of both polyhedrons.

Considering the final configuration where rigid squares A, B and C, formed by vertices A_i, B_i and C_i, (i = 1, 2, 3 and 4), respectively, are orthogonal to each other, the revolute axes at A_2, B_2, C_2 should be

$$\begin{aligned}
\mathbf{s}_{A2} &= (-\frac{3}{2},\ \frac{1-2\sqrt{2}}{2},\ -\frac{\sqrt{2}+1}{2})^T, \\
\mathbf{s}_{B2} &= (-\frac{\sqrt{2}+1}{2}, -\frac{3}{2}, \frac{1-2\sqrt{2}}{2})^T, \\
\mathbf{s}_{C2} &= (-\frac{\sqrt{2}+1}{2},\ -\frac{3}{2},\ \frac{1-2\sqrt{2}}{2})^T.
\end{aligned} \quad [3]$$

The detailed derivation can be found in SI: Section S1.1.

Using the symmetry, the hollow $D_1D_2E_1E_2F_1F_2$ that links rigid squares formed by vertices D_i, E_i and F_i, (i = 1, 2, 3 and 4) can also be made to a threefold-symmetric Bricard linkage, Fig. 2(d).

So far, a total of 12 vertices are converted to 1-DOF revolute joints. If the truncated octahedron is treated as a truss with the truss analogy (*19*), the total number of DOF, m, is 2 according to the Maxwell's rule (SM: Section S1.2) as the Kutzbach criterion cannot give the correct DOF for the overconstrained linkage (*17*).

The polyhedron will have threefold symmetry during the transformation, instead of octahedral symmetry, due to the introduction of the Bricard linkages. In addition, the mirror symmetry can be retained should both Bricard linkages are driven simultaneously, Fig. 3(a).

To reduce the overall number of the DOF further, one more spherical joint at a vertex needs to be changed to a joint of other form. We choose to replace one spherical joint with one revolute joint. However, doing so generally cuts the mobility of mechanism to zero for a revolute joint has only one DOF. Since we have already used the overconstrained Bricard linkages, we speculate that the mobility could be retained by placing the revolute joint along a particular direction.

We pick vertex A_3, marked in red in Fig. 2(e), as the location for the revolute joint replacement. Applying the truss analogy again yields $m = 1$ as long as the rotational axis is placed on the plane bisecting angle $\angle A_2A_3E_3$. Considering symmetric nature of the polyhedron, both spherical joints at B_3 and C_3 can be replaced with revolute joints

as well without altering the value of *m*, Fig. 2(f). The detailed analysis can be found in SI: Section S1.3.

Similarly, the spherical joints at D_3, E_3 and F_3 can also be replaced with revolute joints to get a 1-DOF system, but it should be noted that the replacement can only take place at either vertices A_3, B_3 and C_3, or D_3, E_3 and F_3, not concurrently. This can be proven in two ways. The first is to calculate *m*, which turns out to be 0 if a total of six revolute joints are placed. Second, we can also use the relationships amongst the angle variables of the polyhedron to illustrate why only three revolute joints can be used. Consider the case shown in Fig. 2(f) with the rotational axes of revolute joints at A_3, B_3, C_3 pointing to centre of the polyhedron. Figure 3(b) shows that in the 1-DOF polyhedron, the two linkages do not move simultaneously as in the 2-DOF case in Fig. 3(a). Furthermore, Fig. 3(c) depicts δ^A vs. ρ^A, δ^D and ρ^D curves during the transformation, where δ^A and ρ^A, δ^D (= $\angle D_1D_2E_1$) and ρ^D (= $\angle D_2D_1F_1$) are folding angles of two adjacent joints in the Bricard linkages $A_1A_2C_1C_2B_1B_2$ and $D_1D_2E_1E_2F_1F_2$, respectively, as shown in Fig. 2(f) (SM: Section S1.4 illustrates how these curves are obtained). It is clear that generally $\delta^A \neq \delta^D$ and $\rho^A \neq \rho^D$ except at three configurations marked by red dots. Hence, the motion of these two Bricard linkages differs from each other in general during the transformation, which explains why the joint replacement cannot be done at A_3, B_3, C_3 and D_3, E_3, F_3 concurrently.

The introduction of additional revolute joints enables a 1-DOF transformation between a truncated octahedron and its paired octahedron at the cost that the octahedral symmetry is no longer preserved. In other words, the motion of each square is not the same as that in the face rotation-translation transformation. The motion paths of the eight square centres and their normal directions are plotted in Fig. 3(d) with square A being chosen as the driven one which moves along the path in the rotation-translation transformation (SM: Section 1.5). It is clear that the motion paths of other squares deviate from that of square A. However, once the transformation is completed, the truncated octahedron ends up being a cube, and the transformation is threefold-symmetric about the collinear symmetric axis of both Bricard linkages $A_1A_2C_1C_2B_1B_2$ and $D_1D_2E_1E_2F_1F_2$.

A 3D printed prototype has been made that has successfully verified the concept. The transformation sequence of this model is shown in Fig. 3(e) and SM: Video 2.

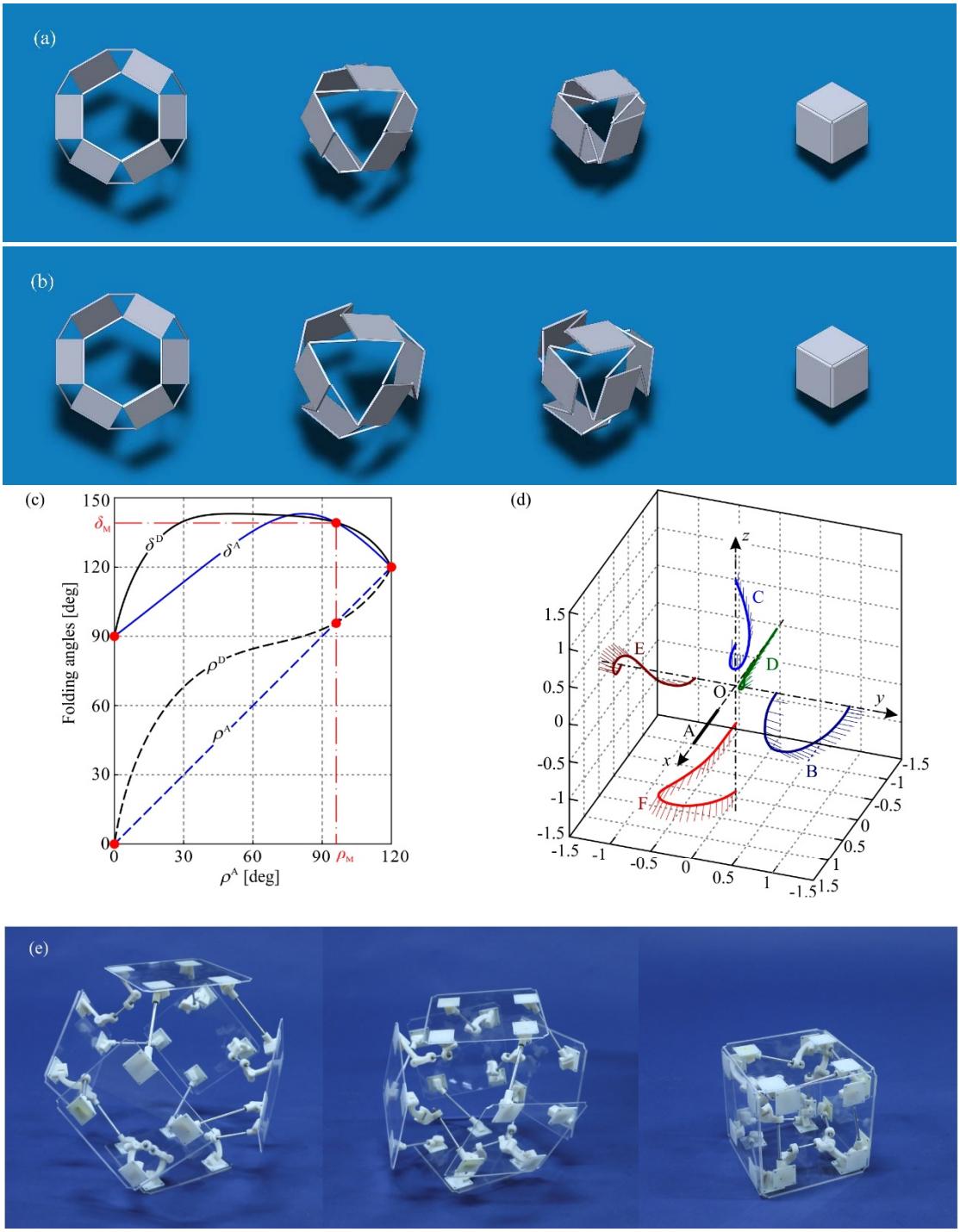

Fig. 3. Transformation sequence and motion paths when a truncated octahedron shrinks to a cube. Deployment sequences of two computer models with (a) 2 DOFs and (b) 1 DOF where ρ^A is 120°, 60°, 30° and 0°, respectively from left to right; (c) relationships amongst folding angles of two threefold-symmetric Bricard linkages $A_1A_2C_1C_2B_1B_2$ and $D_1D_2E_1E_2F_1F_2$ when the truncated octahedron transforms; (d) motion paths of the centres of the rigid square faces and their normals; (e) the transformation sequence between truncated octahedron and cube of a prototype.

Transformation between Truncated Tetrahedron and Tetrahedron

The above approach can also be immediately applied to the transformation between truncated tetrahedron and tetrahedron since again the four rigid triangular faces in the former are connected by bars forming four hexagonal hollows, which could be made to vanish during the transformation. Figures 4(a) – (c) show a process in which the spherical joints at vertices A_1, A_2, B_1, B_2, C_1 and C_2 are replaced by revolute joints with the rotational axes being

$$\begin{aligned} \mathbf{s}_{A1} &= (-3, 1, -1)^{\mathrm{T}}, \quad \mathbf{s}_{A2} = (5, -7, 3)^{\mathrm{T}}, \\ \mathbf{s}_{B1} &= (1, 3, 1)^{\mathrm{T}}, \quad \mathbf{s}_{B2} = (3, -5, -7)^{\mathrm{T}}, \\ \mathbf{s}_{C1} &= (-1, -1, 3)^{\mathrm{T}}, \quad \mathbf{s}_{C2} = (7, -3, -5)^{\mathrm{T}}. \end{aligned} \qquad [4]$$

It produces a threefold-symmetric Bricard linkage $A_1A_2B_1B_2C_1C_2$. In addition, three more revolute joints replace the spherical ones at D_1, D_2 and D_3 whose rotational axes are

$$\mathbf{s}_{D1} = (1, -1, -3)^{\mathrm{T}}, \ \mathbf{s}_{D2} = (3, -1, -1)^{\mathrm{T}}, \ \mathbf{s}_{D3} = (1, -3, -1)^{\mathrm{T}}. \qquad [5]$$

These joint replacement has led to a 1-DOF system. The transformation is threefold-symmetric about the symmetric axis of Bricard linkages $A_1A_2C_1C_2B_1B_2$ which also passes the centre of triangle D, as shown in the transformation sequence of a CAD model Fig. 4(d) (also in SM: Video 3). SI: Section S2 provides further details.

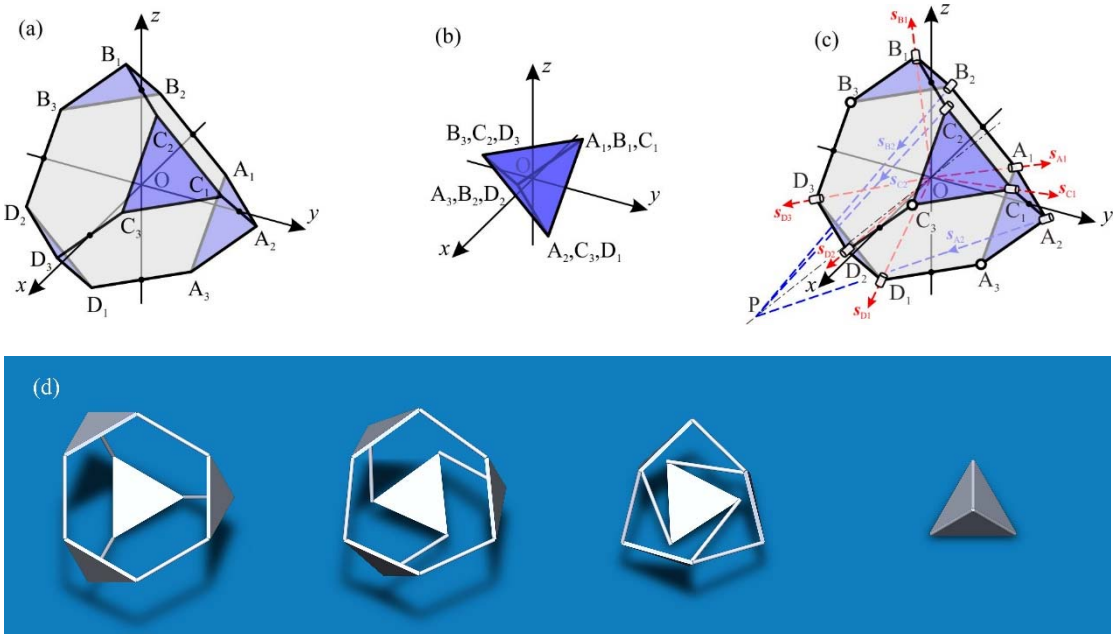

Fig. 4. Joint replacement in truncated tetrahedron and the tetrahedron. (a) The truncated tetrahedron and the Cartesian coordinate system; (b) positions of the vertices when the truncated tetrahedron shrinks to a tetrahedron; (c) revolute joints replace the spherical joints at vertices A_1, A_2, B_1, B_2, C_1 and C_2 leading to a threefold-symmetric Bricard linkage, and further joint replacements at D_1, D_2, D_3 result in a 1-DOF system; (d) the motion sequence of a CAD model in symmetric view.

Transformation between Cuboctahedron and Octahedron

Both the cuboctahedron and octahedron have eight rigid triangular faces, but unlike the truncated tetrahedron or truncated octahedron, the hollows are square, Fig. 1(b). No longer can the Bricard linkage be used to fold up the hollows during the transformation. Instead, the other overconstrained linkage, the Bennett linkage, is to be adopted. Note that the Bennett linkage is the only spatial 4*R* linkage (20).

Both the cuboctahedron and octahedron are also octahedral symmetric, Fig. 5(a) and (b), and the transformation from the former to the latter can be done by moving together vertices A and I, B and D, C and K, E and F, G and H as well as J and L, respectively. If four revolute joints replace the spherical joints at A, B, C and D, respectively, hollow ABCD can be made as a Bennett 4*R* linkage provided that rotational axes of these joints are arranged in such a way that ensures the geometrical conditions governing its motion are met. The directions of the axes at A and B are

$$\mathbf{s}_{\mathrm{A}} = [\frac{\sqrt{5}}{5}, 0, -\frac{2\sqrt{5}}{5}]^{\mathrm{T}}, \quad \mathbf{s}_{\mathrm{B}} = [0, -\frac{2\sqrt{5}}{5}, -\frac{\sqrt{5}}{5}]^{\mathrm{T}}, \qquad [6]$$

respectively, and other two axes at C and D can be obtained by symmetric rotation as illustrated in Fig. 5(c). Meanwhile, due to symmetry, triangular faces IJE, JKF, KLG, LIH can be connected by another Bennett 4*R* linkage IJKL similar to the Bennett linkage ABCD, Fig. 5(d). The truss analogy of this polyhedral linkage yields an overall DOF $m = 1$ according to the Maxwell's rule. No further replacement of spherical joints is needed.

The nature of mirror symmetry connotes that both Bennett linkages ABCD and IJKL always take the same configuration during the transformation. The relationships between the folding angles δ and ρ, which are marked in Fig. 5(d), are shown in Fig. 5(e). Figure 5(f) depicts motion paths of the triangular face centres and their normal directions with face ABE chosen as the driven element. It indicates that the octahedral symmetry is also broken during the transformation but the three orthogonal plane symmetry is maintained, see Fig. 5(g). A prototype has been made with rigid metal faces and hinge joints, whose transformation sequence is shown in Fig. 5(h) and SM: Video 4. The detailed design and kinematic analysis can be found in SI: Section S3, respectively.

CONCLUSION

In this paper, we have proposed the kinematic method to accomplish 1-DOF shape transformation between paired Platonic solids and Archimedean solids using 4*R* and 6*R* spatial linkages. The method has successfully resulted in three transformable polyhedrons. The transformations always end with the targeted polyhedral shapes, though some symmetries of the original polyhedrons are broken during transformation. An analysis of the singular values of the equilibrium matrix for each polyhedron in its truss form has shown that the minimum value always remains zero, whereas the rest never deduce to zero. This observation indicates that motion can take place without any bifurcation. Since our approach is purely a kinematic one using robust hinges, any relatively rigid materials can be used for manufacturing the parts. The transformations are both material and loading independent, and can be repeated again and again.

We envisage that our method could be applied to other paired polyhedrons. For instance, a 1-DOF transformation may be realized for the transformation between truncated cube and octahedron by folding those hollows in the octagon with 8*R* spatial linkages. 8*R* linkage in general would have more than one DOF. Whether a number of such interlinked linkages could lead to a single DOF spatial tiling, is a challenge remains to be tackled.

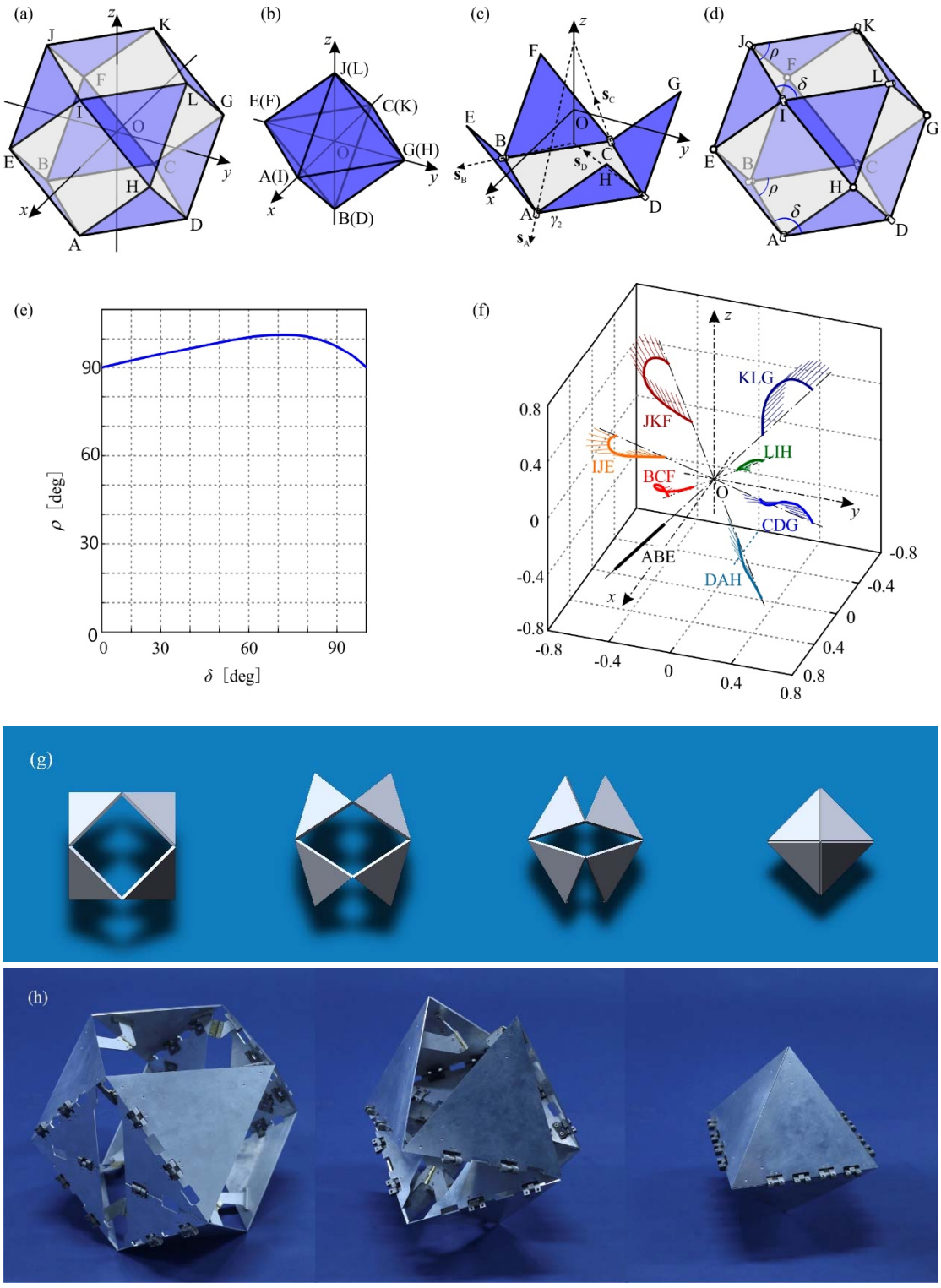

Fig. 5. Transformation between cuboctahedron and octahedron. (a) a cuboctahedron and the Cartesian coordinate system; (b) positions of the vertices when the cuboctahedron shrinks to a octahedron; (c) a Bennett 4*R* linkage is introduced to realize the transformation of four triangular faces, and axes of revolute joints; (d) two Bennett linkages, ABCD and IJKL, connected by four spherical joints at vertices E, F, G, and H, which makes the cuboctahedron a 1-DOF system; (e) relationships between folding angles of two Bennett linkages; (f) motion paths of the triangular face centres and their normals; (g) symmetric view of the polyhedral transformation; (h) the

transformation sequence of a prototype where the rigid triangular faces are made of metal sheet and the revolute joints are made of common door hinges.

MATERIALS AND METHODS

The mathematical derivations were outlined in detail in the supplementary text. All physical models were made from relative rigid materials to demonstrate the mechanism motions. The prototype demonstrating the transformation between a truncated octahedron and a cube (shown in Fig. 3e and video S2) consisted of square facets and bars connected by joints. The facets were cut from 3mm thick acrylic panels by a CNC milling machine. The bars had diameter of 5mm, and they were made from aluminum alloy 6061. The hinges and their supports were produced using a Stratasys Dimension Elite 3D printing machine with ABS plus P430 supplied by Stratasys. The spherical joints (ball joints) were replaced by three revolute joints whose axes met at the points where the centres of spherical joints should be. The other prototype demonstrating the transformation between a cuboctahedron and an octahedron (shown in Fig. 5h and video S4) had triangular facets cut from 2mm thick aluminum alloy 6061 sheets with a CNC milling machine. The hinges on the edges of facets were made from stainless steel 304 produced with a wire-electrode cutting machine. Conventional brass butt hinges were used for the hinges at vertices. The hinge supporters were machined out of aluminum alloy 6061.

The deployment of the two prototypes was done by hand. During the transformation, no visible material deformation was detected. It was expected that the centre positions of each facets would track the motion paths of the mathematical models shown in Figs. 3d and 5f, respectively.

All of the simulations (shown in Figs. 3a and d, 4d and 5g as well as videos S1 and S3) were done using SolidWorks 2014.

SUPPLEMENTARY MATERIALS

Supplementary Text

video S1. Simulation of rotation and translation between an octahedron and a cuboctahedron using cylindrical joints.

video S2. A prototype constructed to demonstrate the transformation between a truncated octahedron and a cube.

video S3. Simulation of transformation between a truncated tetrahedron and a tetrahedron.

video S4. A prototype constructed to demonstrate the transformation between cuboctahedron and octahedron.

REFERENCES

1. P. Cromwell, *Polyhedrons*, pp 51-94, (The Press Syndicate of the University of Cambridge, 1997),.
2. R. Skelton, Tensegrity Approaches to in-space construction of a 1g growable habitat. *the NASA Innovative Advanced Concepts (NIAC) Program's 2016 Symposium*. (Raleigh, NC, Aug. 22-25, 2016).
3. Ames Research Center, Small spacecraft technology state of the art. *NASA/TP-2015-216648/REV1.* (2015).
4. R. Buckminster Fuller, *No more secondhand God and other writings* (Anchor Books, New York, 1971)
5. J. D. Clinton, *Advanced structural geometry studies, part II. a geometric transformation concept for expanding rigid structures.* (Southern Illinois University, NASA Report CR-1735, Washington D. C., 1971).
6. R. Buckminster Fuller, *Synergetics: explorations in the geometry of thinking* (MacMillan, New York, 1997).
7. J. Shim, C. Perdigou, F. R.Chen, K. Bertoldi, P. M. Reis, Buckling-induced encapsulation of structured elastic shells under pressure. *Proceedings of the National Academic of Science of the United States of America* 109:5978-5983 (2012).
8. H. Stachel, Zwei bemerkenswerte bewegliche Strukturen. *Journal of Geometry* 43(1-2):14-21, (1992).
9. H. F. Verheyen, The complete set of Jitterbug transformers and the analysis of their motion. *Computers & Mathematics with Applications* 17(1–3):203-250, (1989).

10. S. K. Agrawal, S. Kumar, M. Yim, Polyhedral single degree-of-freedom expanding structures: design and prototypes. *J Mech Design* 124(3):473-478, (2002).
11. C. Hoberman, Geared expanding structures. *US Patent 20,040,134,157*, (2004).
12. C. M. Gosselin, D. Gagnon-Lachance, Expandable polyhedral mechanisms based on polygonal one-degree-of-freedom faces. *Proceedings of the Institution of Mechanical Engineers, Part C: Journal of Mechanical Engineering Science* 220(7):1011-1018, (2006).
13. T. Laliberté, C. M. Gosselin, Polyhedrons with articulated faces. *Proceedings of the 12th IFToMM World Congress, Besançon, June*, pp 18-21, (2007).
14. G. Wei, J. S. Dai, Synthesis and construction of a family of one-DOF highly overconstrained deployable polyhedral mechanisms (DPMs). in *ASME 2012 International Design Engineering Technical Conferences and Computers and Information in Engineering Conference* (Chicago, IL), (2012).
15. G. Kiper, E. Söylemez, Regular polygonal and regular spherical polyhedral linkages comprising Bennett loops. *Computational Kinematics*, eds Kecskeméthy A & Müller A (Springer Berlin Heidelberg), pp 249-256, (2009).
16. H. S. M. Coxeter, *Regular Polytopes*, pp 46-47, (Methuen Publishing Ltd, London, 1948).
17. G. Gogu G, Mobility of mechanisms: a critical review. *Mech Mach Theory* 40(9):1068-1097, (2005).
18. Y. Chen, Z. You, T. Tarnai, Threefold-symmetric Bricard linkages for deployable structures. *Int. J. Solids Struct.* 42(8):2287-2301, (2005).
19. F. Yang, Y. Chen, R. Kang, J Ma, Truss transformation method to obtain the non-overconstrained forms of 3D overconstrained linkages. *Mech Mach Theory* 102:149-166, (2016).
20. J. S. Beggs, *Advanced Mechanism* (Macmillan Company, New York, 1966).

Acknowledgments

Funding: Chen thanks the support of the National Natural Science Foundation of China (Projects 51290293 and 51422506) and the Ministry of Science and Technology of China (Project 2014DFA70710). Z You wishes to acknowledge the support of Air Force Office of Scientific Research (FA9550-16-1-0339). He was a visiting professor at Tianjin University during the course of this research. **Author contributions:** YC and ZY conceived and supervised the research. FY did initial mathematical modelling and made the prototypes. YC and ZY then verified all the derivations. All authors wrote the manuscript. **Competing interests:** The authors declare that they have no competing interests. **Data and materials availability:** All data needed to evaluate the conclusions in the paper are present in the paper and/or the Supplementary Materials. Additional data related to this paper may be requested from the authors.

Transformation of Polyhedrons - Supplementary Text

Yan Chen[1,2*], Fufu Yang[1], Zhong You[1,3*]

Author affiliation:

[1] School of Mechanical Engineering, Tianjin University, Tianjin 300072, China

[2] Key Laboratory of Mechanism Theory and Equipment Design of Ministry of Education, Tianjin University, Tianjin 300072, China

[3] Department of Engineering Science, University of Oxford, Parks Road, Oxford, OX1 3PJ, UK

* Corresponding authors (Chen's email: yan_chen@tju.edu.cn, You's email: zhong.you@eng.ox.ac.uk).

S1. Transformation between Truncated Octahedron and Cube

S1.1 Introduction of the Threefold Symmetric Bricard 6*R* Linkages

The transformation between truncated octahedron and cube is better illustrated by the positions of the vertices using the Cartesian coordinate system shown in Fig. 2(a) and (b). If each side of the polyhedrons has unit length, the positions of the vertices of the truncated octahedron are

$$
\begin{aligned}
&A_1^{to}=(\sqrt{2},\frac{\sqrt{2}}{2},0)^T,\ A_2^{to}=(\sqrt{2},0,\frac{\sqrt{2}}{2})^T,\ A_3^{to}=(\sqrt{2},-\frac{\sqrt{2}}{2},0)^T,\ A_4^{to}=(\sqrt{2},0,-\frac{\sqrt{2}}{2})^T,\\
&B_1^{to}=(0,\sqrt{2},\frac{\sqrt{2}}{2})^T,\ B_2^{to}=(\frac{\sqrt{2}}{2},\sqrt{2},0)^T,\ B_3^{to}=(0,\sqrt{2},-\frac{\sqrt{2}}{2})^T,\ B_4^{to}=(-\frac{\sqrt{2}}{2},\sqrt{2},0)^T,\\
&C_1^{to}=(\frac{\sqrt{2}}{2},0,\sqrt{2})^T,\ C_2^{to}=(0,\frac{\sqrt{2}}{2},\sqrt{2})^T,\ C_3^{to}=(-\frac{\sqrt{2}}{2},0,\sqrt{2})^T,\ C_4^{to}=(0,-\frac{\sqrt{2}}{2},\sqrt{2})^T,\\
&D_1^{to}=(-\sqrt{2},0,-\frac{\sqrt{2}}{2})^T,\ D_2^{to}=(-\sqrt{2},-\frac{\sqrt{2}}{2},0)^T,\ D_3^{to}=(-\sqrt{2},0,\frac{\sqrt{2}}{2})^T,\ D_4^{to}=(-\sqrt{2},\frac{\sqrt{2}}{2},0)^T,\\
&E_1^{to}=(-\frac{\sqrt{2}}{2},-\sqrt{2},0)^T,\ E_2^{to}=(0,-\sqrt{2},-\frac{\sqrt{2}}{2})^T,\ E_3^{to}=(\frac{\sqrt{2}}{2},-\sqrt{2},0)^T,\ E_4^{to}=(0,-\sqrt{2},\frac{\sqrt{2}}{2})^T,\\
&F_1^{to}=(0,-\frac{\sqrt{2}}{2},-\sqrt{2})^T,\ F_2^{to}=(-\frac{\sqrt{2}}{2},0,-\sqrt{2})^T,\ F_3^{to}=(0,\frac{\sqrt{2}}{2},-\sqrt{2})^T,\ F_4^{to}=(\frac{\sqrt{2}}{2},0,-\sqrt{2})^T,
\end{aligned}
\qquad [S1]
$$

where superscript "to" is for the truncated octahedron. For the cube, the vertices positions are

$$
\begin{aligned}
&A_1^c = B_1^c = C_1^c = (\frac{1}{2},\frac{1}{2},\frac{1}{2})^T,\ B_4^c = C_2^c = D_3^c = (-\frac{1}{2},\frac{1}{2},\frac{1}{2})^T,\\
&C_3^c = D_2^c = E_4^c = (-\frac{1}{2},-\frac{1}{2},\frac{1}{2})^T,\ A_2^c = C_4^c = E_3^c = (\frac{1}{2},-\frac{1}{2},\frac{1}{2})^T,\\
&A_4^c = B_2^c = F_3^c = (\frac{1}{2},\frac{1}{2},-\frac{1}{2})^T,\ B_3^c = D_4^c = F_2^c = (-\frac{1}{2},\frac{1}{2},-\frac{1}{2})^T,\\
&D_1^c = E_1^c = F_1^c = (-\frac{1}{2},-\frac{1}{2},-\frac{1}{2})^T,\ A_3^c = E_2^c = F_4^c = (\frac{1}{2},-\frac{1}{2},-\frac{1}{2})^T,
\end{aligned}
\qquad [S2]
$$

in which superscript "c" represents the cube.

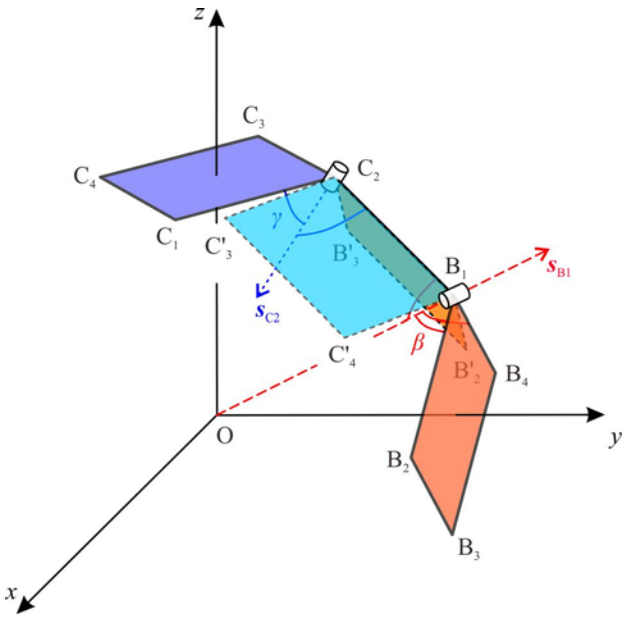

Fig. S1. Directions of the rotational axes of the revolute joints at B_1 and C_2.

Now we replace the spherical joints at vertices A_1, A_2, C_1, C_2, B_1 and B_2 with revolute joints. To enable the hexagonal hollow $A_1A_2C_1C_2B_1B_2$ to vanish during the transformation, the three rigid square surfaces and three bars must form a threefold-symmetric Bricard 6*R* linkage. Determination of the rotational axes of revolute joints at A_1, B_1 and C_1 is illustrated in the main paper, which yields

$$
\mathbf{s}_{B1} = (0, \sqrt{2}, \frac{\sqrt{2}}{2})^T. \qquad [S3]
$$

The angles between the axis $\mathbf{s}_{B1}$ and side B_1C_2 can be calculated as

$$
\beta = \arccos(\frac{\mathbf{s}_{B1} \cdot \overrightarrow{C_2^{to}B_1^{to}}}{|\mathbf{s}_{B1}|}) = \arccos(\frac{\sqrt{10}}{10}) = 71.57°. \qquad [S4]
$$

In order to determine $\mathbf{s}_{C2}$, the direction of the rotational axis at C_2, let us fix the side B_1C_2. Square faces B and C of the truncated octahedron then rotate about $\mathbf{s}_{B1}$ and $\mathbf{s}_{C2}$, and arrive at their

final positions (lightly shaded), respectively. Vertex B_4 reaches to C_2 indicating that $B_4' = C_2^{to}$ (the prime represented the final position), and B_1^{to} remains where it was. This rotation can be obtained by applying a transformation matrix

$$\mathbf{T} = \begin{bmatrix} -\frac{2}{3} & -\frac{1}{3} & \frac{2}{3} \\ \frac{1}{3} & \frac{2}{3} & \frac{2}{3} \\ -\frac{2}{3} & \frac{2}{3} & -\frac{1}{3} \end{bmatrix}. \quad [S5]$$

The positions of B_2 after rotation is, therefore,

$$B_2' = \mathbf{T}B_2^{to} = (-\frac{2\sqrt{2}}{3}, \frac{5\sqrt{2}}{6}, \frac{\sqrt{2}}{3})^T. \quad [S6]$$

On the other hand, the rotation of the square face C about $\mathbf{s}_{C2}$ gives $C_1' = B_1^{to}$, and $C_2' = C_2^{to}$ as C_2^{to} remains at the same position. After the rotation, squares B and C form two faces of the cube, which leads to

$$\overrightarrow{C_1'C_4'} \perp \overrightarrow{C_1'C_2'} \text{ and } \overrightarrow{C_1'C_4'} \perp \overrightarrow{B_1'B_2'}, \quad [S7]$$

Thus,

$$\overrightarrow{B_1^{to}C_4'} = \overrightarrow{B_1^{to}C_2^{to}} \times \overrightarrow{B_1^{to}B_2'} \quad [S8]$$

which gives

$$C_4' = (\frac{1}{3}, \sqrt{2} - \frac{2}{3}, \frac{\sqrt{2}}{2} - \frac{2}{3})^T \quad [S9]$$

Now we can calculate the direction of the axis of the revolute joint at C_2, which is

$$\mathbf{s}_{C2} = \overrightarrow{C_1^{to}B_1^{to}} \times \overrightarrow{C_4^{to}C'} = (\frac{1-2\sqrt{2}}{2}, -\frac{\sqrt{2}+1}{2}, -\frac{3}{2})^T \quad [S10]$$

The angles between $\mathbf{s}_{C2}$ and side C_2B_1 is

$$\gamma = \arccos(\frac{\overrightarrow{C_2^{to}B_1^{to}} \cdot \mathbf{s}_{C2}}{|\mathbf{s}_{C2}|}) = 84.42° \quad [S11]$$

We can obtain other rotational axis directions of the revolute joints using symmetry, resulting in

$$\mathbf{s}_{A1}=(\sqrt{2},\frac{\sqrt{2}}{2},0)^{T},\ \mathbf{s}_{C1}=(\frac{\sqrt{2}}{2},0,\sqrt{2})^{T},$$
$$\mathbf{s}_{A2}=(-\frac{3}{2},-\frac{\sqrt{2}+1}{2},\frac{1-2\sqrt{2}}{2})^{T},\ \text{and}\ \mathbf{s}_{B2}=(\frac{1-2\sqrt{2}}{2},-\frac{3}{2},-\frac{\sqrt{2}+1}{2})^{T}. \quad [S12]$$

As the geometries of both hexagonal hollows $D_1D_2E_1E_2F_1F_2$ and $A_1A_2C_1C_2B_1B_2$ are identical and they are not connected directly, the hexagonal hollow $D_1D_2E_1E_2F_1F_2$ can also be set as the same Bricard linkage by replacing the spherical joints at vertices D_1, D_2, E_1, E_2, F_1 and F_2 with revolute ones. Subsequently axes of its joints are

$$\mathbf{s}_{D1}=(-\sqrt{2},0,-\frac{\sqrt{2}}{2})^{T},\ \mathbf{s}_{E1}=(-\frac{\sqrt{2}}{2},-\sqrt{2},0)^{T},\ \mathbf{s}_{F1}=(0,-\frac{\sqrt{2}}{2},-\sqrt{2})^{T},$$
$$\mathbf{s}_{D2}=(\frac{3}{2},-\frac{1-2\sqrt{2}}{2},\frac{\sqrt{2}+1}{2})^{T},\ ,\mathbf{s}_{E2}=(\frac{\sqrt{2}+1}{2},\frac{3}{2},-\frac{1-2\sqrt{2}}{2})^{T}, \quad [S13]$$
$$\mathbf{s}_{F2}=(-\frac{1-2\sqrt{2}}{2},\frac{\sqrt{2}+1}{2},\frac{3}{2})^{T}.$$

By now by replacing twelve spherical joints with revolute joints, the truncated octahedron has had two threefold-symmetric Bricard 6*R* linkages.

S1.2 The Truss Analogy

Mobility calculation of a spatial mechanism can become rather difficult especially when it is overconstrained because of the complex geometry. The truss analogy (*S1*) is a convenient way forward. The analogy converts a spatial assembly into a truss and uses the equilibrium matrix to determine kinematic indeterminacy (*S2*). In the truss analogy, the rigid parts (links) are converted into a line, triangle or tetrahedron, a revolute joint is modelled as a pair of spherical joints along the rotational axis of the revolute joint, unit length is generally chosen as the distance between these spherical joints, and the rest of spherical joints remain unchanged. For instance, the revolute joint at A_1 shown in Fig. S2(a) equals to two spherical joints at A_1 and a_1, which is placed at a unit distance apart along $\mathbf{s}_{A1}$, bar B_1C_2 is converted to the tetrahedron $B_1b_1C_2c_2$. According to this approach, a threefold-symmetric Bricard linkage formed by three rigid squares and three rigid bars, shown in Fig. S2(a), could be transformed to its truss form shown in Fig. S2(b) (*S3*).

For a spatial truss consisting of b bars and j joints, its equilibrium equations has the form of

$$\mathbf{Ht}=\mathbf{p} \quad [S14]$$

where $\mathbf{H}$ is the $3j \times b$ equilibrium matrix, $\mathbf{t}$ is a $b \times 1$ vector of bar forces, and $\mathbf{p}$ is the $3j \times 1$ vector of nodal load components. According to the Maxwell's rule, the kinematic indeterminacy is

$$m=3j-r-6 \quad [S15]$$

where r is the rank of the equilibrium matrix $\mathbf{H}$, and 6 is for the rigid body motion of the entire truss.

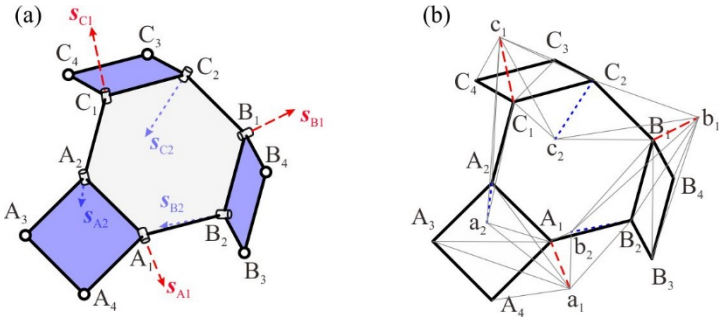

Fig. S2. Applying the truss analogy to the truncated octahedron with Bricard linkages.
(a) a portion of the truncated octahedron containing a threefold-symmetric Bricard 6*R* linkage;
(b) the kinematically equivalent truss form.

The kinematic indeterminacy of an overconstrained polyhedronsl mechanism can now be calculated using Eq. [S15].

After two Bricard linkages are introduced into the truncated octahedron, a total of twelve vertices are converted to revolute joints and the rest remain to be spherical joints. Applying the truss analogy gives $b = 126$ and $j = 42$ joints, and the rank of the equilibrium matrix $r = 118$, which gives a total DOF $m = 2$.

S1.3 Introduction of additional revolute joints to obtain a one-DOF polyhedron

To reduce the number of the DOF from 2 to 1, one more spherical joint needs to be replaced with a revolute joint. Let us place a revolute joint at vertex A_3, Fig. S3.

Since vertex E_3 will move towards A_2 during transformation, the rotational axis of the revolute joint at A_3 must be in the plane bisecting angle $\angle A_2A_3E_3$. Now the assembly has 13 revolute joints and 11 spherical joints. Using the truss analogy, it has $b = 130$, $j = 43$ and $r = 122$, which gives a total DOF $m = 1$ according to Eq. [S15].

Due to the threefold rotational symmetry of the polyhedronsl linkage after two Bricard linkages are introduced, it is obvious that B_3 and C_3 should all be replaced with revolute joints like A_3, whose rotational axes are determined by symmetric operations from the rotational axis at A_3. m remains to be 1 after these operations.

As mentioned previously, the rotational axis of the revolute joint at A_3 must be in the plane bisecting angle $\angle A_2A_3E_3$. This condition alone does not completely define the direction of the axis. Angle ζ_{A3}, which is the deviation angle of the rotational axis from the line linking A_3 to the centre of the polyhedron, is used to determine the precise direction of the rotation axis of the revolute joint, Fig. S3. The angle's positive direction is defined by the right-hand rule with the right thumb pointing along a line parallel to E_3A_2. It can be shown that ζ_{A3} can take any value without changing the overall

m. The selection of this angle is governed by the condition that no interference is allowed during the shape transformation. It can be shown that if

$$-60.9° < \zeta_{A3} < 19.5°, \qquad \text{[S16]}$$

no physical intersection occurs.

The prototype in the main paper adopts a particular parameter, $\zeta_{A3} = 0$, which means that revolute joint axis at A_3 pointing towards the body centre of the polyhedron. Those at B_3, C_3 are placed in the same way.

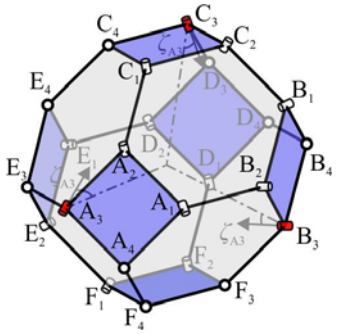

Fig. S3. Additional revolute joints are introduced at A_3, B_3 and C_3 (shown in red).

S1.4 Kinematic relationships amongst rotational variables of the Bricard linkages

In the threefold symmetric Bricard linkage $A_1A_2C_1C_2B_1B_2$, the rotational axes of the revolute joint are not orthogonal to the edge of the rigid square faces or bars (links), and thus it is a linkage in its alternative form (S3). The kinematic relationships in terms of the linkage variables θ and φ of the Bricard linkage using the D-H notation (*S4*) has already been given by Chen et. al. (S3) where the link lengths are set to be the shortest distances spanning two adjacent rotational axes. Now we try to convert the linkage variables to the folding angles that can be physically inspected during transformation.

Figure S4(a) shows the threefold symmetric Bricard linkage and the link lengths are displayed in Fig. S4(b) where the positions of the points that give the link lengths are denoted by A_{b1}, B_{b1}, ..., etc.. OP is the symmetric axis of the linkage. At each point, a coordinate system (denoted by x_1 and z_1, x_2 and z_2, ..., etc., respectively) is established based on the D-H notation. The link lengths are

$$C_{b1}C_{b2} = C_{b2}B_{b1} = B_{b1}B_{b2} = B_{b2}A_{b1} = A_{b1}A_{b2} = A_{b2}C_{b1} = l, \qquad \text{[S17]}$$

and the other distances are

$$A_{b1}A_1 = B_{b1}B_1 = C_{b1}C_1 = c, \text{ and } A_{b2}A_2 = B_{b2}B_2 = C_{b2}C_2 = d. \qquad \text{[S18]}$$

Denote by δ and ρ the folding angles at A_1, (also B_1 and C_1) and A_2 (also B_2 and C_2), respectively, and by α and $2\pi-\alpha$ the twist angles between x_6 and x_1 (also between x_2 and x_3, x_4 and x_5) and between x_1 and x_2 (also between x_3 and x_4, x_5 and x_6), respectively. According to Eq. [S12],

$$\alpha = 2\pi - \arccos\left(\frac{\mathbf{s}_{B2}\cdot\mathbf{s}_{A1}}{|\mathbf{s}_{B2}||\mathbf{s}_{A1}|}\right) = 2\pi - \arccos\left(-\frac{5\sqrt{5}+2\sqrt{10}}{5\sqrt{21-2\sqrt{2}}}\right) = 214.79^\circ \qquad [S19]$$

Geometrically we have

$$l^2 = 1-c^2-d^2-2cd\cos\alpha,\ l^2+d^2 = c^2+1-2c\cos\beta,$$
$$l^2+c^2 = d^2+1-2d\cos\gamma, \qquad [S20]$$

taking the side length of the polyhedron is 1. Noting that β, γ and α are obtained known from Eqs. [S4], [S11] and [S19], we have

$$c = \frac{\cos\beta-\cos\alpha\cos\gamma}{\sin^2\alpha} = 1.22\ ,\ d = \frac{\cos\gamma-\cos\alpha\cos\beta}{\sin^2\alpha} = 1.10 \qquad [S21]$$

and

$$l = \sqrt{\frac{\sin^2\alpha-\cos^2\beta-\cos^2\gamma+2\cos\alpha\cos\beta\cos\gamma}{\sin^2\alpha}} = 0.71 \qquad [S22]$$

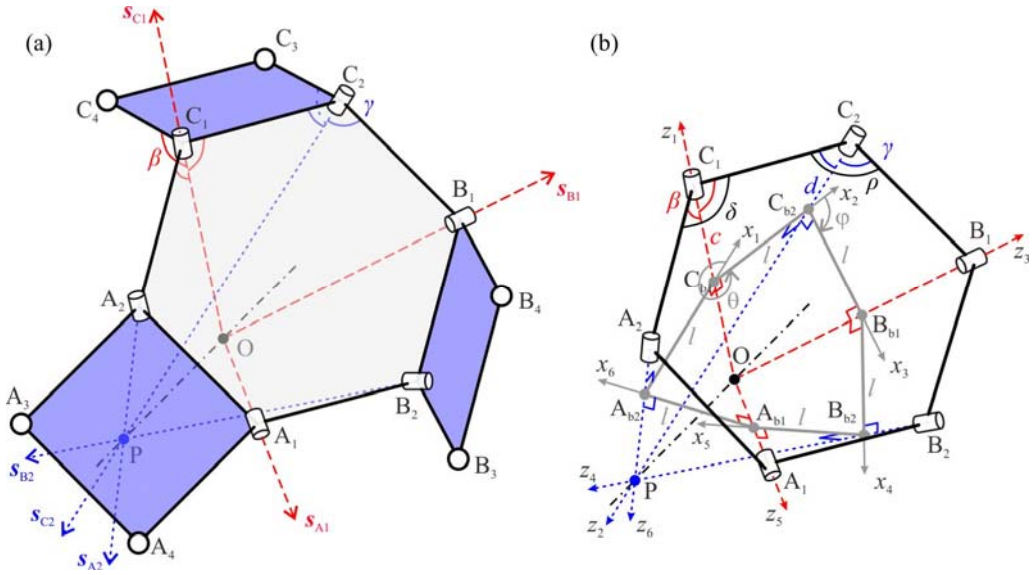

Fig. S4. (a) The hexagon $A_1A_2C_1C_2B_1B_2$ formed by squares A, B, C and (b) the threefold symmetric Bricard 6*R* linkage $A_{b1}A_{b2}C_{b1}C_{b2}B_{b1}B_{b2}$ illustrated with thick gray lines.

Hence, using the coordinate system x_2, y_2 and z_2 at C_{b2}, the following positions can be found,

$$\begin{gathered} C_{b2} = (0, 0, 0)^T,\ C_2 = (0, 0, -d)^T,\ B_{b1} = (l\cos\varphi, l\sin\varphi, 0)^T, \\ B_1 = (l\cos\varphi - c\sin\alpha\sin\varphi, l\sin\varphi + c\sin\alpha\cos\varphi, c\cos\alpha)^T, \\ C_{b1} = (-l, 0, 0)^T,\ C_1 = (-l, c\sin\alpha,\ c\cos\alpha)^T. \end{gathered} \quad [S23]$$

which yields

$$\overrightarrow{B_1C_1} = (-l\cos\varphi + c\sin\alpha\sin\varphi - l, c\sin\alpha - l\sin\varphi - c\sin\alpha\cos\varphi, 0)^T \quad [S24]$$

Using triangle $B_1C_1C_2$ we can find

$$|\overrightarrow{B_1C_1}| = 2\sin(\rho/2). \quad [S25]$$

Combining Eqs. [S24] and [S25] results in

$$\cos\rho = 1 - [l^2(1+\cos\varphi) + c^2\sin^2\alpha(1-\cos\varphi) - 2lc\sin\alpha\sin\varphi] \quad [S26]$$

Similarly, the relationship between θ and δ can also be obtained, which is

$$\cos\delta = 1 - [l^2(1+\cos\theta) + d^2\sin^2\alpha(1-\cos\theta) - 2ld\sin\alpha\sin\theta] \quad [S27]$$

Initially for the truncated octahedron,

$$\delta^{to} = \rho^{to} = \frac{2\pi}{3} \quad [S28]$$

During the transformation, ρ decreases from $\rho^{to} = \frac{2\pi}{3}$ when the polyhedron is a truncated octahedron, to $\rho^c = 0$ when it becomes a cube, whilst δ increases from $\delta^{to} = \frac{2\pi}{3}$ at first, and then decreases to $\delta^c = \frac{\pi}{2}$. The corresponding linkage variables are

$$\theta^{to} = 34.8°,\ \theta^c = 166.12°,\ \varphi^{to} = 147.49°,\ \varphi^c = 268.0°. \quad [S29]$$

S1.5 Plotting Motion Paths Using the Predictor-corrector Algorithm

Although analytical solution of kinematics is the best way to describe the motion of a mechanism, the kinematic equations can be rather difficult to solve. To deal with this problem, a numerical approach, known as the predictor-corrector algorithm, was proposed by Kumar and Pellegrino (*S5*). It is capable of detecting bifurcation points with singular values of equilibrium matrices. This algorism has been used to plot the motion paths of the centres of the rigid square faces.

S2. Transformation of Truncated Tetrahedron and Tetrahedron

Using the Cartesian coordinate system shown in Fig. 4(a), positions of all vertices of the truncated tetrahedron can be obtained as follows.

$$\begin{gathered}
A_1^{tt}=(-\frac{3}{\sqrt{8}},\frac{1}{\sqrt{8}},-\frac{1}{\sqrt{8}})^T,\ A_2^{tt}=(-\frac{1}{\sqrt{8}},\frac{3}{\sqrt{8}},-\frac{1}{\sqrt{8}})^T,\ A_3^{tt}=(-\frac{1}{\sqrt{8}},\frac{1}{\sqrt{8}},-\frac{3}{\sqrt{8}})^T,\\
B_1^{tt}=(-\frac{1}{\sqrt{8}},-\frac{1}{\sqrt{8}},\frac{3}{\sqrt{8}})^T,\ B_2^{tt}=(-\frac{3}{\sqrt{8}},-\frac{1}{\sqrt{8}},\frac{1}{\sqrt{8}})^T,\ B_3^{tt}=(-\frac{1}{\sqrt{8}},-\frac{3}{\sqrt{8}},\frac{1}{\sqrt{8}})^T,\\
C_1^{tt}=(\frac{1}{\sqrt{8}},\frac{3}{\sqrt{8}},\frac{1}{\sqrt{8}})^T,\ C_2^{tt}=(\frac{1}{\sqrt{8}},\frac{1}{\sqrt{8}},\frac{3}{\sqrt{8}})^T,\ C_3^{tt}=(\frac{3}{\sqrt{8}},\frac{1}{\sqrt{8}},\frac{1}{\sqrt{8}})^T,\\
D_1^{tt}=(\frac{1}{\sqrt{8}},-\frac{1}{\sqrt{8}},-\frac{3}{\sqrt{8}})^T,\ D_2^{tt}=(\frac{1}{\sqrt{8}},-\frac{3}{\sqrt{8}},-\frac{1}{\sqrt{8}})^T,\ D_3^{tt}=(\frac{3}{\sqrt{8}},-\frac{1}{\sqrt{8}},-\frac{1}{\sqrt{8}})^T.
\end{gathered} \tag{S30}$$

in which the superscript "tt" represents the truncated tetrahedron. After transformation, the truncated tetrahedron becomes the tetrahedron shown in Fig. 4(b). The positions of the vertices are now

$$\begin{gathered}
A_1^{te}=B_1^{te}=C_1^{te}=(-\frac{1}{\sqrt{8}},\frac{1}{\sqrt{8}},\frac{1}{\sqrt{8}})^T,\ A_3^{te}=B_2^{te}=D_2^{te}=(-\frac{1}{\sqrt{8}},-\frac{1}{\sqrt{8}},-\frac{1}{\sqrt{8}})^T,\\
A_2^{te}=C_3^{te}=D_1^{te}=(\frac{1}{\sqrt{8}},\frac{1}{\sqrt{8}},-\frac{1}{\sqrt{8}})^T,\ B_3^{te}=C_2^{te}=D_3^{te}=(\frac{1}{\sqrt{8}},-\frac{1}{\sqrt{8}},\frac{1}{\sqrt{8}})^T.
\end{gathered} \tag{S31}$$

where the superscript "t" is for the tetrahedron.

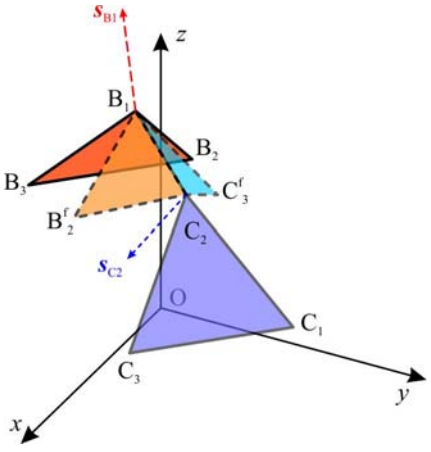

Fig. S5. A portion of the truncated tetrahedron showing relative motion of two triangles $B_1B_2B_3$ and $C_1C_2C_3$ linked by bar B_1C_2 for the determination of revolute joint axes.

Now we convert the hexagonal hollow $A_1A_2C_1C_2B_1B_2$ to a threefold-symmetric Bricard 6*R* linkage by replacing spherical joints at A_1, A_2, C_1, C_2, B_1 and B_2 with revolute joints as we did previously. Letting the rotational axes of revolute joints on A_1, B_1 and C_1 pointing toward the centre of the truncated tetrahedron, Fig. S5, we have

$$\mathbf{s}_{A1} = (-3, 1, -1)^{\mathrm{T}},\ \mathbf{s}_{B1} = (-1, -1, 3)^{\mathrm{T}},\ \mathbf{s}_{C1} = (1, 3, 1)^{\mathrm{T}}. \quad [S32]$$

In order to determine the direction of the revolute joint at C_2, we fix the side B_1C_2. During transformation, triangle $B_1B_2B_3$ rotates about $\mathbf{s}_{B1}$ during the transformation and the final position of B_3, denoted by B_3', will coincide with C_2, i.e., $B_3' = C_2^{tt}$. This rotation can therefore obtained by a transformation matrix

$$\mathbf{T} = \begin{bmatrix} -\frac{2}{3} & -\frac{1}{3} & -\frac{2}{3} \\ \frac{2}{3} & -\frac{2}{3} & -\frac{1}{3} \\ -\frac{1}{3} & -\frac{2}{3} & \frac{2}{3} \end{bmatrix} \quad [S33]$$

The final position of B_2 becomes

$$B_2' = \mathbf{T}B_2^{tt} = (\frac{5\sqrt{2}}{12}, -\frac{5\sqrt{2}}{12}, -\frac{7\sqrt{2}}{12})^{\mathrm{T}} \quad [S34]$$

In the tetrahedron, dihedral angle between two adjacent triangles is $\arccos(\frac{1}{3})$, and thus, the final position of C_3 can be calculated as

$$C_3' = (\frac{\sqrt{2}}{36}, -\frac{\sqrt{2}}{36}, \frac{5\sqrt{2}}{36})^{\mathrm{T}} \quad [S35]$$

Meanwhile, considering rotation of triangle $C_1C_2C_3$ about C_2, the final position of C_1 coincides with B_1^{tt}, i.e., $C_1' = B_1^{tt}$. Hence, the axis of the revolute joint on C_2 is

$$\mathbf{s}_{C2} = \overrightarrow{C_1^{tt}C_1'} \times \overrightarrow{C_3^{tt}C'_3} = (\frac{1}{2}, -\frac{5}{6}, -\frac{7}{6})^{\mathrm{T}} \quad [S36]$$

The other axes can be obtained by symmetric rotations

$$\mathbf{s}_{A2} = (\frac{5}{6}, -\frac{7}{6}, -\frac{1}{2})^{\mathrm{T}},\ \mathbf{s}_{B2} = (\frac{7}{6}, -\frac{1}{2}, -\frac{5}{6})^{\mathrm{T}}. \quad [S37]$$

Placing a single Bricard linkage alone cannot transform the truncated tetrahedron to a 1-DOF mechanism. There are still six spherical joints at vertices A_3, B_3, C_3 and D_1, D_2, D_3, respectively. Considering the threefold symmetry of this polyhedronsl linkage, we can convert either joints at A_3,

B_3, C_3, or at D_1, D_2, D_3 to revolute joints with the rotational axes pointing towards the centre of the polyhedron. The polyhedron after this convention has 1 DOF based on the truss analogy.

S3. Transformation between Cuboctahedron and Octahedron

S3.1 Introduction of the Bennett 4*R* Linkages

With the Cartesian coordinate system shown in Fig. 5(a), the vertices of the cuboctahedron are

$$\begin{gathered}
A^{co}=(\frac{\sqrt{2}}{2},0,-\frac{\sqrt{2}}{2})^{T},\ B^{co}=(0,-\frac{\sqrt{2}}{2},-\frac{\sqrt{2}}{2})^{T},\ C^{co}=(-\frac{\sqrt{2}}{2},0,-\frac{\sqrt{2}}{2})^{T},\\
D^{co}=(0,\frac{\sqrt{2}}{2},-\frac{\sqrt{2}}{2})^{T},\ E^{co}=(\frac{\sqrt{2}}{2},-\frac{\sqrt{2}}{2},0)^{T},\ F^{co}=(-\frac{\sqrt{2}}{2},-\frac{\sqrt{2}}{2},0)^{T},\\
G^{co}=(-\frac{\sqrt{2}}{2},\frac{\sqrt{2}}{2},0)^{T},\ H^{co}=(\frac{\sqrt{2}}{2},\frac{\sqrt{2}}{2},0)^{T},\ I^{co}=(\frac{\sqrt{2}}{2},0,\frac{\sqrt{2}}{2})^{T},\\
J^{co}=(0,-\frac{\sqrt{2}}{2},\frac{\sqrt{2}}{2})^{T},\ K^{co}=(-\frac{\sqrt{2}}{2},0,\frac{\sqrt{2}}{2})^{T},\ L^{co}=(0,\frac{\sqrt{2}}{2},\frac{\sqrt{2}}{2})^{T}.
\end{gathered} \tag{S38}$$

For the octahedron, the positions of the vertices are, under the Cartesian coordinate system shown in Fig. 5(b),

$$\begin{gathered}
A^{o}=I^{o}=(\frac{\sqrt{2}}{2},0,0)^{T},\ B^{o}=D^{o}=(0,0,-\frac{\sqrt{2}}{2})^{T},\ C^{o}=K^{o}=(-\frac{\sqrt{2}}{2},0,0)^{T},\\
E^{o}=F^{o}=(0,-\frac{\sqrt{2}}{2},0)^{T},\ G^{o}=H^{o}=(0,\frac{\sqrt{2}}{2},0)^{T},\ J^{o}=L^{o}=(0,0,\frac{\sqrt{2}}{2})^{T}.
\end{gathered} \tag{S39}$$

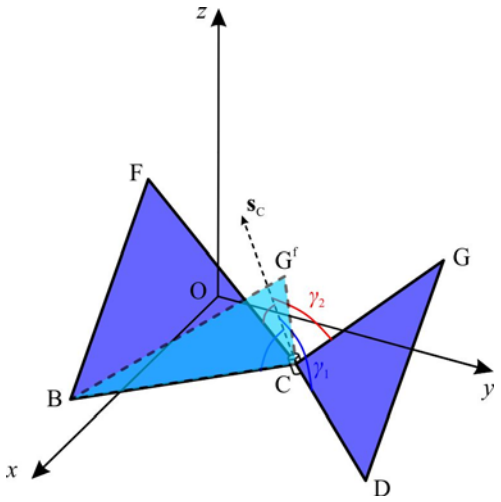

Fig. S6. A portion of the cuboctahedron showing relative motion of two adjacent triangles BCF and CDG for the determination of revolute joint axes.

The hollows in the cuboctahedron have square shapes. As the Bennett 4*R* linkage is the only linkage with four links, we set square hollow ABCD to a Bennett linkage by converting the spherical joints at vertices A, B, C and D to revolute joints, Fig. S6. To decide the directions of the rotational axes of the revolute joints, let us fix triangular face BCF. Denote by $\mathbf{s}_C$ axis of the revolute joint at G. The triangular face CDG will rotate about $\mathbf{s}_C$. D and G will reach B and G′ at the end of the transformation. Meanwhile, triangle BCF and BCG′ should form two adjacent faces of the octahedron, and thus, position of G′ can be obtained by roation of F about BC by the angle $\arccos(-\frac{1}{3})$, which is the dihedral angle of adjacent triangles in the octahedron. Hence,

$$\mathrm{G}' = (\frac{\sqrt{2}}{6}, \frac{\sqrt{2}}{6}, -\frac{\sqrt{2}}{3})^{\mathrm{T}}, \tag{S40}$$

Since $\mathbf{s}_C$ must be in both planes bisecting angles $\angle$DCB and $\angle$GCG′, we have

$$\mathbf{s}_C \perp \mathrm{D}^{co}\mathrm{B}^{co} \text{ and } \mathbf{s}_C \perp \mathrm{G}^{co}\mathrm{G}'. \tag{S41}$$

Therefore,

$$\mathbf{s}_C = \overrightarrow{\mathrm{D}^{co}\mathrm{B}^{co}} \times \overrightarrow{\mathrm{G}^{co}\mathrm{G}'} = (\frac{2}{3},\ 0,\ \frac{4}{3})^{\mathrm{T}} \tag{S42}$$

The angles between $\mathbf{s}_C$ and the sides CB and CF can be found as

$$\gamma_1 = \arcsin(\frac{\mathbf{s}_C \times \overrightarrow{\mathrm{C}^{co}\mathrm{B}^{co}}}{|\mathbf{s}_C|}) = 71.57°,\ \gamma_2 = \arcsin(\frac{\mathbf{s}_C \times \overrightarrow{\mathrm{C}^{co}\mathrm{F}^{co}}}{|\mathbf{s}_C|}) = 50.77° \tag{S43}$$

According to Euler-Rodrigues formula (*S6*), the rotational axes of the remaining three rovolute joints can also be found as

$$\mathbf{s}_A = (-\frac{2}{3},\ 0,\ \frac{4}{3})^{\mathrm{T}},\ \mathbf{s}_B = (0,\ \frac{4}{3},\ \frac{2}{3})^{\mathrm{T}},\ \mathbf{s}_D = (0, -\frac{4}{3},\ \frac{2}{3})^{\mathrm{T}}. \tag{S44}$$

To convert the cuboctahedron to a single DOF mechanism, an additional Bennett linkage needs to be used for the symmetric hollow IJKL. The directions of the revolute joints are

$$\begin{aligned} &\mathbf{s}_I = (-\frac{2}{3}, 0, -\frac{4}{3})^{\mathrm{T}},\ \mathbf{s}_J = (0, \frac{4}{3}, -\frac{2}{3})^{\mathrm{T}}, \\ &\mathbf{s}_K = (\frac{2}{3}, 0, -\frac{4}{3})^{\mathrm{T}},\ \mathbf{s}_L = (0, -\frac{4}{3}, -\frac{2}{3})^{\mathrm{T}}. \end{aligned} \tag{S45}$$

Now the polyhedron contains two Bennett linkages, whose links are all triangular faces, and these two linkages are connected by four spherical joints at vertices E, F, G and H. The truss analogy shows that $m = 1$.

S3.2 Relationship between geometric parameters and kinematic variables

The kinematic relationships in terms of the linkage variables θ and φ of the Bennett linkage using the D-H notation has already been given by Beggs (*S7*) where the link lengths are set to be the shortest distances spanning two adjacent rotational axes. Now we try to convert the linkage variables to the folding angles that can be physically inspected during transformation.

In the cuboctahedron to octahedron transformation, the Bennett linkage, which could be either hollows ABCF or IJKL, is an equilateral one because of the nature of the polyhedrons, i.e., all the lengths of this linkage are the same, which is denoted by l, and the twist angles are α and $\pi - \alpha$, respectively. The relationship between the linkage variables θ and φ is, therefore,

$$\tan\frac{\theta}{2}\tan\frac{\varphi}{2} = \frac{1}{\cos\alpha}. \qquad [S46]$$

The revolute axes of the Bennett linkages in the cuboctahedron are not perpendicular to their connecting links, which means that the linkages are of the alternative forms of the Bennett linkage. Chen and You (*S8*) provided a comprehensive set of geometrical relationships between the parameters of the original Bennett linkage and those of its alternative form. In the following, we follow the same step to obtain the kinematic relation between the angular variables.

Both the alternative form and its original Bennett linkage of quadrilateral ABCD are illustrated in Fig. S7, where $A_bB_bC_bD_b$ is the original. Meanwhile, $\mathbf{s}_A$ and $\mathbf{s}_C$ meet at M, $\mathbf{s}_B$ and $\mathbf{s}_D$ meet at N, and $\boldsymbol{z}$ is set as the symmetric axis of the mechanism which crosses A_bC_b and B_bD_b at their midpoints P and Q, respectively. Denote by c and d the distances AA_b and BB_b, respectively. It can be found that (*S8*),

$$l = \left|\overrightarrow{A_bB_b}\right| = \frac{\sqrt{42}}{14} = 0.46\,, \qquad [S47]$$

$$c = \left|\overrightarrow{AA_b}\right| = \frac{3\sqrt{10}}{14} = 0.68\,, \qquad [S48]$$

$$d = \left|\overrightarrow{BB_b}\right| = \frac{2\sqrt{10}}{7} = 0.90\ . \qquad [S49]$$

$$\alpha = \arccos\left(\frac{\mathbf{s}_A\cdot\mathbf{s}_B}{|\mathbf{s}_A|\cdot|\mathbf{s}_B|}\right) = \arccos 0.4 = 66.42^\circ\,. \qquad [S50]$$

The kinematic relationship between θ and φ, given by Eq. [S46], is completely established once α is known. Moreover,

$$\cos\angle A_bMC_b = -\cos\angle A_bPC_b = 2\frac{1+\cos\varphi}{1-\cos\theta} - 1 \qquad [S51]$$

$$\left|\overrightarrow{\mathrm{A_bM}}\right|^2 = \frac{l^2(1+\cos\varphi)(1-\cos\theta)}{-2(\cos\theta+\cos\varphi)} \quad [S52]$$

$$\cos\angle \mathrm{B_bND_b} = 2\frac{1+\cos\theta}{1-\cos\varphi} - 1, \quad [S53]$$

$$\left|\overrightarrow{\mathrm{B_bN}}\right|^2 = \frac{l^2(1+\cos\theta)(1-\cos\varphi)}{-2(\cos\theta+\cos\varphi)}, \quad [S54]$$

$$\left|\overrightarrow{\mathrm{AC}}\right|^2 = 2\left|\overrightarrow{\mathrm{AM}}\right|^2(1-\cos\angle \mathrm{A_bMC_b}) = 2\left(\left|\overrightarrow{\mathrm{A_bM}}\right| + c\right)^2(1-\cos\angle \mathrm{A_bMC_b}), \quad [S55]$$

$$\left|\overrightarrow{\mathrm{BD}}\right|^2 = 2\left|\overrightarrow{\mathrm{BN}}\right|^2(1-\cos\angle \mathrm{B_bND_b}) = 2\left(-\left|\overrightarrow{\mathrm{B_bN}}\right| + d\right)^2(1-\cos\angle \mathrm{B_bND_b}), \quad [S56]$$

Considering Eqs. [S53] and [S54],

$$\left|\overrightarrow{\mathrm{BD}}\right|^2 = 4\left(d + \sqrt{\frac{(1+\cos\theta)(1-\cos\varphi)}{-2(\cos\theta+\cos\varphi)}}\,l\right)^2\left(\frac{\cos\theta+\cos\varphi}{\cos\varphi-1}\right). \quad [S57]$$

Then,

$$\delta = \arccos\left(1 - \frac{\left|\overrightarrow{\mathrm{BD}}\right|^2}{2}\right) \quad [S58]$$

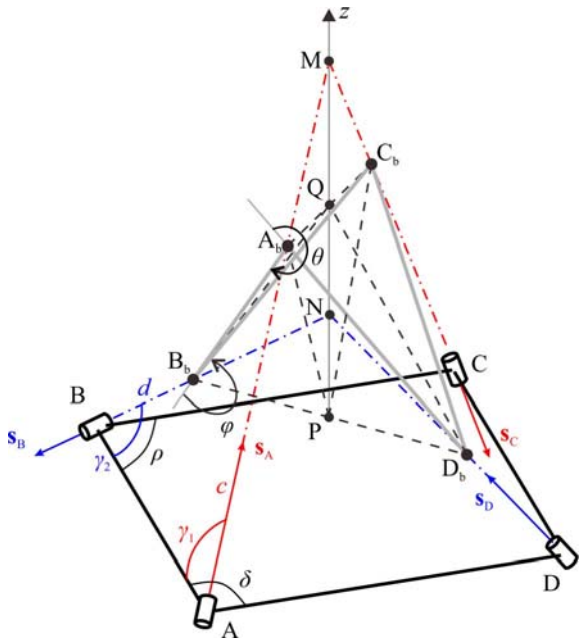

Fig. S7. The geometirc relationship between Bennett linkage, $A_bB_bC_bD_b$, and its alternative form, ABCD which is used as quadrilaterals in the depolyable polyhedron.

Similarly,

$$\rho = \arccos\left(1 - \frac{\left|\overrightarrow{\mathrm{AC}}\right|^2}{2}\right) \tag{S59}$$

where

$$\left|\overrightarrow{\mathrm{AC}}\right|^2 = 4\left(c + \sqrt{\frac{(1+\cos\varphi)(1-\cos\theta)}{-2(\cos\theta+\cos\varphi)}}l\right)^2\left(\frac{\cos\theta+\cos\varphi}{\cos\theta-1}\right). \tag{S60}$$

Therefore, the relationship between folding angles, δ and ρ, and kinematic variables θ and φ, can be obtained using Eqs. [S57-S60]. By now, the relationship between kinematic variables, given by Eq. [S46], can be converted to that between the angular variables δ and ρ, which is plotted in Fig. 5(e).

During the transformation, δ decreases from $\frac{\pi}{2}$ when the polyhedron is a cuboctahedron, to 0 when it becomes an octahedron, whilst ρ increases from $\frac{\pi}{2}$ initially, and subsequently decreases back to $\frac{\pi}{2}$. The corresponding linkage kinematic variables at the start and end of the transformation are

$$\begin{gathered}\theta^{\mathrm{co}} = 2\arctan\left(-2\sqrt{5}\right) = -154.79^\circ,\ \varphi^{\mathrm{co}} = 2\arctan\left(-\frac{\sqrt{5}}{4}\right) = -58.41^\circ \\ \theta^{\mathrm{o}} = \varphi^{\mathrm{co}},\ \varphi^{\mathrm{o}} = \theta^{\mathrm{co}}.\end{gathered} \tag{S61}$$

References

S1. F. Yang, Y. Chen, R. Kang, J. Ma J, Truss transformation method to obtain the non-overconstrained forms of 3D overconstrained linkages. *Mech Mach Theory* 102:149-166, (2016)

S2. S. Pellegrino, C. R. Calladine, Matrix analysis of statically and kinematically indeterminate frameworks. *Int. J. Solids Struct.* 22(4):409-428, (1986).

S3. Y. Chen, Z. You, T. Tarnai, Threefold-symmetric Bricard linkages for deployable structures. *Int. J. Solids Struct.* 42(8):2287-2301, (2005).

S4. J. Denavit, R. S. Hartenberg, A kinematic notation for lower-pair mechanisms based on matrices. *Trans. ASME J. Appl. Mech.* 22:215-221, (1955).

S5. P. Kumar, S. Pellegrino, Computation of kinematic paths and bifurcation points. *Int. J. Solids Struct.* 37(46-47):7003-7027, (2000).

S6. J. S. Dai, *Geometrical Foundations and Screw Algebra for Mechanisms and Robotics* (Higher Education Press, Beijing, also *Screw Algebra and Kinematic Approaches for Mechanisms and Robotics*, Springer, London, 2014).

S7. J. S. Beggs, *Advanced Mechanism* (Macmillan Company, New York, 1966).

S8. Y. Chen, Z. You, Square deployable frames for space applications: Part I: theory. *Proceedings of the IMechE Part G: Journal of Aerospace Engineering*. 220, 2006, 347-354, (2006).